Collapse of the $Ia\bar{3}d$ cubic symmetry by uniaxial stretching of a double-gyroid block copolymer

Shinichi Sakurai,[1,*] Daisuke Isobe,[1] Shigeru Okamoto,[2] Takeshi Yao,[3] and Shunji Nomura[1]
[1]*Department of Polymer Science and Engineering, Kyoto Institute of Technology, Matsugasaki, Sakyo-ku, Kyoto 606-8585, Japan*
[2]*Department of Material Science and Engineering, Nagoya Institute of Technology, Gokiso-cho, Showa-ku, Nagoya 466-8555, Japan*
[3]*Department of Fundamental Energy Science, Graduate School of Energy Science, Kyoto University, Yoshida, Sakyo-ku, Kyoto 606-8501, Japan*

(Received 24 October 2000; revised manuscript received 25 January 2001; published 17 May 2001)

We report an experimental observation of collapse of the $Ia\bar{3}d$ symmetry by stretching of an elastomeric block copolymer that forms a double-gyroid (DG) microdomain structure. Some new diffraction spots were observed for a deformed DG structure. These spots were assigned to {110} and {200} reflections. For the $Ia\bar{3}d$ symmetry, these reflections are prohibited by the extinction rule and therefore none of them appeared for the sample before deformation. Appearance of these reflections indicates breakdown of the extinction rule and can be explained as a result of collapse of the symmetry of glide when three-dimensional DG networks are partially ruptured upon stretching.

DOI: 10.1103/PhysRevE.63.061803 PACS number(s): 61.41.+e, 61.10.−i, 81.30.−t, 82.70.Kj

I. INTRODUCTION

Dynamic structural reorganization in soft matter such as amphiphilic molecules [1] and block copolymers [2] has been attracting general interests in physics, and various different kinds of supermolecular structures have been found in microemulsions of amphiphilic molecules and microphase-separated structures of block copolymers. The $Ia\bar{3}d$ cubic symmetry was first reported by Luzzati and co-workers [3–5] for a supermolecular structure in amphiphilic microemulsions. Recently, block copolymers were found to form a similar supermolecular structure [6,7]. The minor component of a block copolymer aggregates in three-armed continuous struts that form a three-dimensionally interconnected network with the $Ia\bar{3}d$ symmetry in the matrix of the major component of the block copolymer [8]. Since two independent sets of the three-dimensional (3D) network were found to be interwoven, the morphology is referred to as double gyroid (DG). Dynamic structural reorganization of the DG structure has been studied both in amphiphilic molecules [9–14] and block copolymers [8,15,16], in which these materials undergo transformation from (to) structures with another type of symmetry to (from) the DG structure with the $Ia\bar{3}d$ cubic symmetry. Structural reorganization in amphiphilic molecules under shear flow [14] has been recently studied because of the advantage of a considerably low critical energy to retain the gyroid structures as compared to the block copolymer system. The lower critical energy required for the structural reorganization, in turn, explains that there are no reports of deformation of the gyroid structure in the amphiphilic systems. On the other hand, the DG structure in block copolymers has recently been found to be deformed when thermoplastic elastomers such as polystyrene-*block*-polybutadiene-*block*-polystyrene triblock copolymers are uniaxially stretched [17]. We report here an experimental observation of collapse of the $Ia\bar{3}d$ symmetry by uniaxial stretching, as revealed by two-dimensional small-angle x-ray scattering (2D SAXS). Some diffraction spots were observed for a deformed DG structure as a result of collapse of the extinction rule for the original $Ia\bar{3}d$ symmetry. Although transformation of packing symmetry of crystals is well known in inorganic crystals or metallic alloys that undergo transformation from the NaCl arrangement to the CsCl type under high pressure [18], collapse of symmetry due to fracture is a rare case for a supermolecular structure in soft matter.

II. EXPERIMENTAL SECTION

The SBS triblock copolymer with $M_n = 8.5 \times 10^4$, $M_w/M_n = 1.05$, and $\phi_{PS} = 0.32$ was used where M_n and M_w denote the number- and weight-average molecular weights, respectively, and ϕ_{PS} is the volume fraction of polystyrene (PS) blocks. A toluene solution of this sample with ca. 5 wt % of the initial polymer concentration was cast at room temperature. After complete evaporation of the solvent for about 7 days, an as-cast film obtained was then thermally annealed at 190 °C for about 24 h to form a well-ordered DG structure. The microphase-separated structures were analyzed by using the 2D SAXS technique with synchrotron x rays at BL-10C SAXS beamline (PF, Tsukuba, Japan) with a point-focused incident beam that was collimated by a bent cylindrical mirror [15], and also at BL-45XU SAXS beamline (SPring-8, Nishi-Harima, Japan) with a point-focused beam collimated by a *K-B* type focusing mirror system consisting of horizontal and vertical mirrors [19]. Imaging plates with $250 \times 200\ mm^2$ size and $100 \times 100\ \mu m^2$ resolution were utilized as a detector at the BL-10C SAXS station of PF, while an x-ray image intensifier equipped with a cooled 2D CCD camera was used at the BL-45XU SAXS station of SPring-8. Typical exposure time was 1–4 sec for the imag-

*Author to whom correspondence should be addressed. Email address: shin@ipc.kit.ac.jp

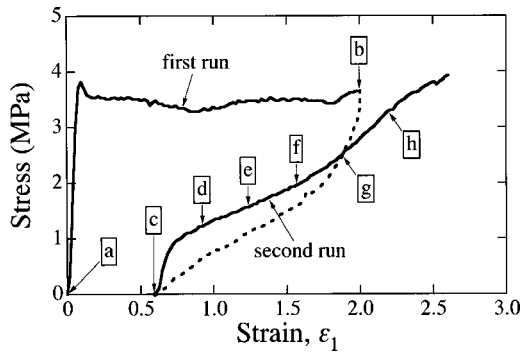

FIG. 1. Stress-strain curve for a DG sample measured at a strain rate of 0.056 sec^{-1}. The first run of the stretching of the virgin DG sample is conducted up to $\varepsilon_1=2.0$. Here, ε_1 designates strain for the first run of stretching, as defined by $\varepsilon_1=(l-l_0)/l_0$, with l_0 $(=15\,\mathrm{mm})$ and l being, respectively, longitudinal lengths of the virgin and stretched films. From $\varepsilon_1=2.0$, the strain was in turn reversed until the stress reached zero. The stress recorded during this process is shown in a dotted curve. Right after this process, the second run of the stretching was performed.

ing plates (PF), and ca. 0.1 sec for 2D CCD camera (SPring-8).

III. RESULTS AND DISCUSSION

The DG sample exhibited the elastomeric property of which the stress-strain curve at a strain rate of 0.056 sec^{-1} is presented in Fig. 1. The first run of the stretching of the virgin DG sample up to $\varepsilon=2.0$ is shown in a thick solid curve. Here, ε_1 designates strain for the first run of stretching as defined by $\varepsilon_1=(l-l_0)/l_0$, with $l_0(=15\,\mathrm{mm})$ and l being, respectively, longitudinal lengths of the virgin and stretched films. A steep increase in the stress was found at the initial stage of the stretching, and necking of the sample film took place. These facts indicate rupture of gyroid networks comprising the glassy PS component. From a slope of the curve in the range $0<\varepsilon_1<0.08$, the tensile modulus is evaluated as 51.4 MPa. Beyond the yielding point the stress is almost constant up to $\varepsilon_1=2.0$, at which the necking propagated thoroughly over the sample film. Then the strain was in turn reversed until the stress reached zero. The stress recorded during this process is shown in a dotted curve. The residual strain ε_r is found to be 0.6. Right after this process, the second run of the stretching was performed, which is shown in a thick solid curve. Again a steep increase in the stress was observed and the tensile modulus evaluated is 10.4 MPa, which is about one-fifth of that for the virgin sample. The steep increase in the stress might suggest additional rupture of the glassy gyroid networks. However, no yielding, no necking, and extremely lower stress in the second run as compared to the first run rather imply deformation of the residual gyroid networks without further rupture. In the course of the reversing strain, rearrangement of the residual gyroid network may take place and deformation of thus relaxed gyroid structure may be responsible for the steep increase in the stress at the initial stage of the stretching of the second run.

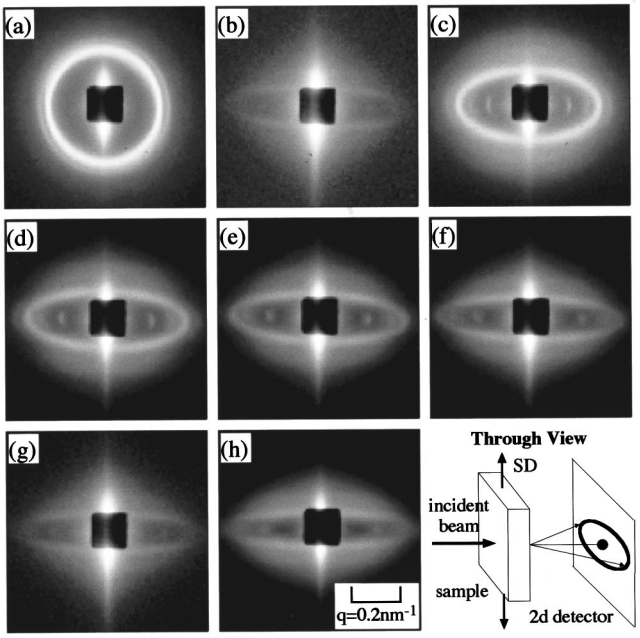

FIG. 2. 2D SAXS pattern (gray-scale displays logarithm of the scattering intensity) of the through view. (a) Virgin film, (b) at $\varepsilon_1=2.0$ from the virgin film, (c) relaxed from $\varepsilon_1=2.0$ (no load but with residual strain $\varepsilon_r=0.8$), and (d)–(h) restretching of the relaxed film at $\varepsilon_2=0.2$, 0.4, 0.6, 0.8, and 1.0, respectively. The value of strain for the second run of stretching, ε_2, was defined with respect to the stretched-and-relaxed film [taking Fig. 2(c) at $\varepsilon_r=0.8$ as a reference and hence $\varepsilon_2=(\varepsilon_1-\varepsilon_r)/(\varepsilon_r+1)$]. Except in Fig. 2(a), the SD is perpendicular to the equator.

Figure 2 shows change in 2D SAXS patterns along with the uniaxial stretching. Labels (a)–(h) in Fig. 1 specify the points where the 2D SAXS measurements were conducted. Note, however, that those are not exactly corresponding to each other because the stress-strain curves were recorded by continuously stretching the sample whereas each 2D SAXS pattern was measured by pinning the sample film at a fixed strain during exposure of x rays. Actually, the values of residual strain are different from each other. The incident x-ray beam was sent to a sample film in such a way that the beam trajectory was parallel to the film normal (so-called through view geometry). Note that intense streaks on the meridian are ascribed to the parasitic scattering from collimation slits. Except in Fig. 2(a), the uniaxial stretching direction (SD) is perpendicular to the equator. The virgin sample exhibits an isotropic pattern with two intense diffraction rings, indicating a randomly oriented polygrain structure. The ratio of radii of these two rings was found to be $\sqrt{6}:\sqrt{8}$. These are assigned to {211} and {220} reflections of the DG structure. Upon the uniaxial stretching of the virgin film, the main {211} reflection was significantly distorted and the {220} reflection completely disappeared [Fig. 2(b)]. Note that the degree of distortion of the {211} reflection can be explained by taking account of deformation of the film at $\varepsilon_1=2.0$. Moreover, the distorted elliptic ring of the {211} reflection is disconnected near the equator, implying disappearance of the {211} planes that are parallel to the SD. These results are in accord with the findings of Dair *et al.* [17]. Since the tensile

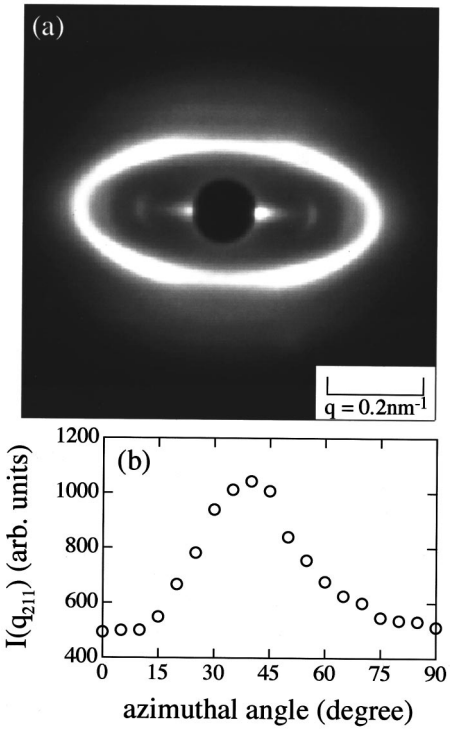

FIG. 3. (a) 2D SAXS result (gray-scale displays the scattering intensity: through view) of a separate measurement at the SPring-8 for the same sample as was used for Fig. 2(c). (b) Variation of the intensity of the {211} diffraction as a function of azimuthal angle. The azimuthal angle is defined with respect to the equator.

stress steeply increased in the initial stage of the stretching, and yielding (viz. necking) was observed [20], the DG structure might lose connectivity of the 3D networks of glassy PS struts. If the PS struts that are oriented parallel to the SD are thoroughly disconnected, the {211} planes parallel to the SD would disappear because such PS struts are placed on those planes.

Figure 2(c) is a result obtained after release of a load from Fig. 2(b) (elongation at $\varepsilon_1=2.0$). Note here that residual strain was $\varepsilon_r=0.8$. By taking account of the residual strain, the degree of distortion of the {211} diffraction ring can be interpreted. As shown in Fig. 3(b), which is converted from a 2D SAXS result [Fig. 3(a)] of a separate measurement at the SPring-8 for the same sample as was used for Fig. 2(c), nontrivial variation of the intensity of the {211} diffraction as a function of azimuthal angle was detected. Here, we defined the azimuthal angle with respect to the equator. The peak is located at 40°, which corresponds to the position of four spots of the {211} diffraction. Since a single crystal of the DG structure gives rise to six spots of the {211} diffraction, the other two spots might appear on the equator in Fig. 2(c). Lack of these two spots on the equator implies that the effect of stretching at $\varepsilon_1=2.0$, i.e., the disappearance of the {211} planes that are parallel to the SD, is still remaining. It is however interesting to observe that the elliptic diffraction ring that was disconnected near the equator in Fig. 2(b) is now reconnected. This fact implies that the ordering regularity of the {211} planes in the equatorial direction is recovered upon release of a load. Although the ordering regularity is

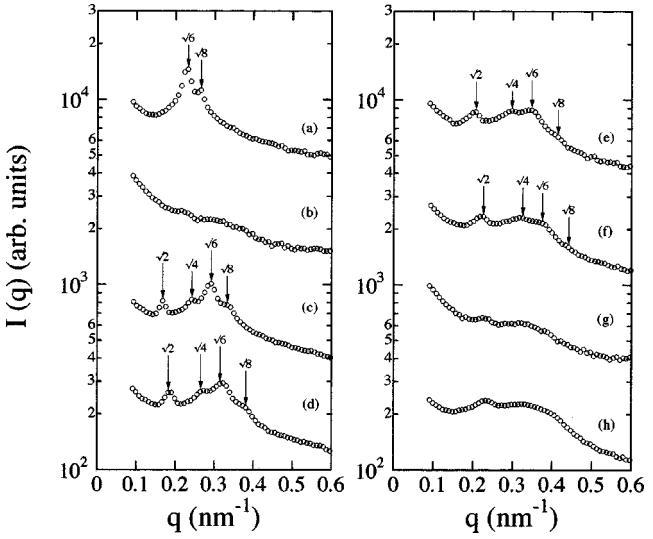

FIG. 4. One-dimensional SAXS profiles reduced from the 2D SAXS patterns shown in Fig. 2.

recovered, some glassy PS struts that had already been ruptured upon the stretching cannot be reconnected at room temperature (below the glass transition temperature of PS). Overall, it turned out that the preferential orientation of the DG structure was induced by the uniaxial stretching and that the orientation remained even in the relaxed film. The orientation was induced such that the {211} planes were placed parallel to the uniaxial stretching direction, giving rise to intense scattering at the azimuthal angle 40° off the equator. Furthermore, it should be noticed that new diffraction spots (more or less arcs) showed up on the equator in Fig. 2(c). We are not sure whether other sets of arcs appeared on the meridian because the beam stopper blocks a low q region. We will come back to a discussion on the new peaks later.

Figures 2(d)–2(h) show change along the process of restretching the film from Fig. 2(c). Note here that the value of strain for the second run of stretching, ε_2, was defined with respect to the stretched-and-relaxed film [taking Fig. 2(c) at $\varepsilon_r=0.8$ as a reference and hence $\varepsilon_2=(\varepsilon_1-\varepsilon_r)/(\varepsilon_r+1)$]. There is no significant change of features and the degree of distortion of the {211} diffraction ring can be explained by taking account of the extent of strain for Figs. 2(d)–2(h).

One-dimensional SAXS profiles, which were reduced from the 2D SAXS patterns by sector averaging with azimuthal angles from $-5°$ to 5° off the equator, are shown in Fig. 4. Here, scattering intensities are plotted in the logarithmic scale and the 1D SAXS profiles were vertically shifted to avoid their overlaps, and q stands for the magnitude of the scattering vector defined as $q=(4\pi/\lambda)\sin(\theta/2)$ with λ and θ being the wavelength of x rays and the scattering angle, respectively. For the virgin film, two distinct peaks labeled with $\sqrt{6}$ and $\sqrt{8}$ were confirmed for the {211} and {220} reflections of the DG structure. Upon stretching up to $\varepsilon_1=2.0$ [Fig. 2(b)], these peaks disappeared. However, these peaks again appeared when the load was removed. Additionally, new peaks labeled with $\sqrt{2}$ and $\sqrt{4}$ showed up. Now, the q positions of all peaks can relatively be assigned to $\sqrt{2}:\sqrt{4}:\sqrt{6}:\sqrt{8}$, suggesting a possibility that the new peaks

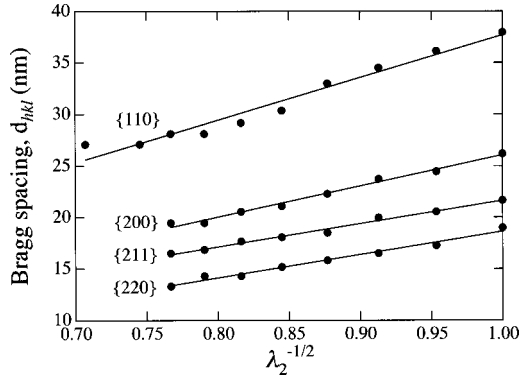

FIG. 5. Variation of d_{hkl} with $\lambda_2^{-1/2}$ for the $\{hkl\}$ planes parallel to the SD.

are ascribed to {110} and {200} reflections. All the peaks are discernible in the course of the successive restretching up to $\varepsilon_2 = 0.6$.

To quantify the shifts of peaks in the course of restretching, we assume the affine deformation with a constant volume of the sample film. Then, the Bragg spacing d_{hkl} ($\equiv 2\pi/q_{hkl}$, where q_{hkl} denotes the peak position of the $\{hkl\}$ reflection) can be expressed by $d_{hkl} = d_{hkl,0}\lambda_2^{-1/2}$ for the $\{hkl\}$ planes parallel to the SD. Here, $d_{hkl,0}$ denotes the value of d_{hkl} for the stretched-and-relaxed film [taking Fig. 2(b) as a reference], and λ_2 is the elongation ratio defined by $\lambda_2 = l/l_r$ with l_r and l being, respectively, longitudinal lengths of the reference and stretched films. Figure 5 shows the variation of d with $\lambda_2^{-1/2}$. Data points nicely fall on respective straight lines for all the reflections. Thus, it is confirmed that shifts of all peaks including new ones have close correlation. This fact in turn suggests that the new peaks are ascribed to a distorted DG structure that may be composed of partially ruptured 3D networks of glassy PS.

Note that there might still be remaining a possibility of a different type of morphology such as a cylinder phase, resulted by degradation of the DG structure upon stretching. If this would be the case, the newly formed regions of a different morphology would co-exist with the original DG structure and new diffraction peaks would appear. However, such a phase, like a cylinder was not detected by TEM observation [20]. As shown in Fig. 6 (through view), almost the same 2D SAXS pattern as Fig. 2(a) was again observed after the stretched sample was fully annealed at 190 °C for 48 h. This fact suggests that the thermal annealing heals the partially ruptured glassy PS rods, so that the original DG structure was recovered. If a cylinder phase would be induced by the uniaxial stretching, the thermal annealing would make the phase more regular causing their new peaks to be sharper and more intense. The fact that the actual new peaks thoroughly disappeared in Fig. 6 definitely rules out the possibility that the DG structure would partly transform into a new phase such as a cylinder.

Finally, we examine collapse of the extinction rule of the $Ia\bar{3}d$ symmetry for the partially ruptured DG structure. If the lattice is merely distorted, the extinction rule is still active. As is in the well-known case of inorganic crystals or metallic alloys, change in symmetry is essential for the collapse of the

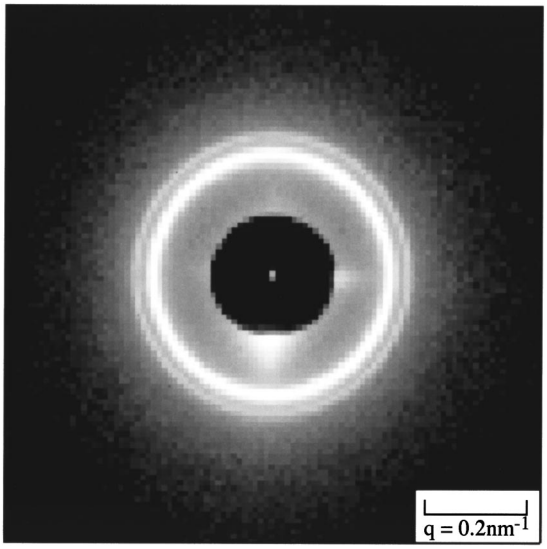

FIG. 6. 2D SAXS pattern (gray-scale displays for logarithm of the scattering intensity; through view) for the stretched sample after fully annealing at 190 °C for 48 h.

extinction rule [18]. In the present case of the DG structure, the glassy PS struts that are parallel to the SD are considered to be ruptured. The relevant extinction rule for the {200} reflection is $h00:h=4n$ (reflection condition), which is due to symmetry with respect to the diamond glide plane [21]. For the {110} reflection, additionally $0kl:k,l=2n$ should also be met, which is ascribed to symmetry with respect to

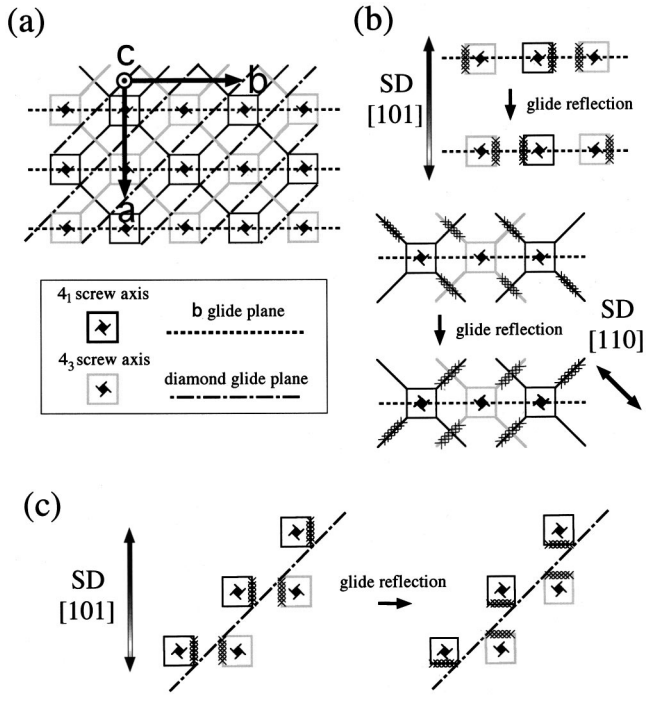

FIG. 7. (a) Unit lattice cell projected along its *c* axis. (b) Drawings explaining the collapse of symmetry with respect to the **b** glide plane for the partially ruptured DG structure. The cross-hatching specifies ruptured rods. (c) Drawing explaining the collapse of symmetry with respect to the diamond glide plane.

the **b** glide plane [21]. Therefore, we examine whether these symmetries are maintained or not in the partially ruptured DG structure. Figure 7 explains the collapse of symmetry of the glide reflection. Figure 7(a) exhibits the unit lattice cell projected along its *c* axis. Here, skeletons of PS networks are drawn and two interwoven sets are distinguished by black and gray lines. The 4_1 and 4_3 screw axes are parallel to the *c* axis in this figure, so that the superposed image contains a bunch of squares. Note that the two neighboring squares in black and gray have screw rotations opposite to each other, while the squares in the same color have the same screw rotation. One rod in the 4_1 and 4_3 screw axes is inclined 45° off the plane on which Fig. 7(a) is drawn. Lines diagonally connecting squares are placed on four different planes parallel to the (001) plane and crossing the *c* axis at $\frac{1}{8}$, $\frac{3}{8}$, $\frac{5}{8}$, and $\frac{7}{8}$. Thus, those lines are all parallel to the plane on which Fig. 7(a) is drawn. Again note that the black and the gray lines have no connection at all. The **b** glide planes and the diamond glide planes are shown as dotted lines and dotted-broken lines, respectively. Figure 7(b) explains the collapse of symmetry with respect to the **b** glide plane for the partially ruptured DG structure. Here, the SD is chosen parallel to the [101] direction, i.e., the direction inclined 45° with respect to the plane on which Fig. 7(b) is drawn. Then the cross-hatched rods that are parallel to the SD may be ruptured. As shown in Fig. 7(b), the structure after the glide reflection with respect to the original **b** glide plane becomes no more the same as that before the glide reflection. Similarly for the SD parallel to the [110] direction, the collapse of symmetry of the glide reflection can be recognized in Fig. 7(b). Figure 7(c) explains the collapse of symmetry with respect to the diamond glide plane with the SD parallel to the [101] direction. With the diamond glide reflection, it is confirmed that the original structure cannot be maintained. If we can assume axisymmetry of the structure with respect to the SD, the (101) reflection should newly appear on the equator and also on the meridian in the through view. Similarly, the (020) reflection should newly appear on the equator as well as the (200) reflection on the lines inclined ca. 45° off the equator in the through view. Thus, the experimentally observed new spots on the equator can be interpreted by taking into account collapse of symmetry of the glide reflection for the partially ruptured DG structure. Our recent TEM studies revealed the partially ruptured DG structure [20].

ACKNOWLEDGMENTS

This work was supported in part by the Grant-in-aid from the Japanese ministry of education, culture, science, and sports, Grant No. 11750781. The research grant from the Mitsubishi Petrochemical Foundation to S.S. is also gratefully acknowledged. The SAXS experiments were performed at the Photon Factory of the Research Organization for High Energy Accelerator with the Approval No. 99G232, and at SPring-8, Proposal No. 1999B0391-ND-np.

[1] *Physics of Amphiphilic Layers*, edited by J. Meunier, D. Langevin, and N. Boccara (Springer-Verlag, New York, 1987).
[2] I. W. Hamley, *The Physics of Block Copolymers* (Oxford University Press, Oxford, 1998).
[3] V. Luzzati *et al.*, Acta Crystallogr. **14**, 660 (1960).
[4] V. Luzzati and P. A. Spegt, Nature (London) **215**, 701 (1967).
[5] V. Luzzati *et al.*, Nature (London) **220**, 485 (1968).
[6] D. A. Hajduk *et al.*, Macromolecules **27**, 4063 (1994).
[7] M. W. Matsen and F. S. Bates, Macromolecules **29**, 1091 (1996).
[8] M. E. Vigild *et al.*, Macromolecules **31**, 5702 (1998).
[9] J. S. Clunie, J. F. Goodman, and P. C. Symons, Trans. Faraday Soc. **65**, 287 (1969).
[10] Y. Rançon and J. Charvolin, J. Phys. Chem. **92**, 2646 (1988).
[11] M. Clerc, A. M. Levelut, and J. F. Sadoc, J. Phys. II **1**, 1263 (1991).
[12] M. Clerc *et al.*, J. Phys. II **5**, 901 (1995).
[13] M. Imai, T. Kato, and D. Schneider, J. Chem. Phys. **106**, 9362 (1997).
[14] M. Imai *et al.*, J. Phys. Chem. Solids **60**, 1313 (1999).
[15] S. Sakurai *et al.*, J. Chem. Phys. **108**, 4333 (1998).
[16] M. W. Matsen, Phys. Rev. Lett. **80**, 4470 (1998).
[17] B. J. Dair *et al.*, Macromolecules **32**, 8145 (1999).
[18] R. W. G. Wyckoff, *Crystal Structures*, 2nd ed. (Wiley, New York, 1963), Vol. 1, p. 105.
[19] T. Fujisawa, J. Jpn. Soc. Synchrotron Radiat. Res. **12**, 194 (1999).
[20] S. Sakurai *et al.* (unpublished).
[21] T. Hahn, *International Tables for Crystallography*, 3rd ed. (Kluwer Academic, Boston, 1992), Vol. A, pp. 706–707.